Dephosphorylation of Iqg1 by Cdc14 regulates cytokinesis in budding yeast

Daniel P. Miller[a], Hana Hall[b], Ryan Chaparian[b], Madison Mara[a], Alison Mueller[a], Mark C. Hall[b], and Katie B. Shannon[a]

[a]Department of Biological Sciences, Missouri University of Science and Technology, Rolla, MO 65401; [b]Department of Biochemistry, Purdue Center for Cancer Research, Purdue University, West Lafayette, IN 47907

ABSTRACT **Cytokinesis separates cells by contraction of a ring composed of filamentous actin (F-actin) and type II myosin. Iqg1, an IQGAP family member, is an essential protein in *Saccharomyces cerevisiae* required for assembly and contraction of the actomyosin ring. Localization of F-actin to the ring occurs only after anaphase and is mediated by the calponin homology domain (CHD) of Iqg1, but the regulatory mechanisms that temporally restrict actin ring assembly are not well defined. We tested the hypothesis that dephosphorylation of four perfect cyclin-dependent kinase (Cdk) sites flanking the CHD promotes actin ring formation, using site-specific alanine mutants. Cells expressing the nonphosphorylatable *iqg1-4A* allele formed actin rings before anaphase and exhibited defects in myosin contraction and cytokinesis. The Cdc14 phosphatase is required for normal cytokinesis and acts on specific Cdk phosphorylation sites. Overexpression of Cdc14 resulted in premature actin ring assembly, whereas inhibition of Cdc14 function prevented actin ring formation. Cdc14 associated with Iqg1, dependent on several CHD-flanking Cdk sites, and efficiently dephosphorylated these sites in vitro. Of importance, the *iqg1-4A* mutant rescued the inability of *cdc14-1* cells to form actin rings. Our data support a model in which dephosphorylation of Cdk sites around the Iqg1 CHD by Cdc14 is both necessary and sufficient to promote actin ring formation. Temporal control of actin ring assembly by Cdk and Cdc14 may help to ensure that cytokinesis onset occurs after nuclear division is complete.**

Monitoring Editor
Daniel J. Lew
Duke University

Received: Dec 22, 2014
Revised: Jun 8, 2015
Accepted: Jun 9, 2015

INTRODUCTION

Cytokinesis, the final step in cell division, divides the cytoplasm between two daughter cells. Precise temporal control is necessary to coordinate cytokinesis and mitosis so that proper chromosome segregation can be completed. Cytokinetic failure results in tetraploid cells, and there is evidence that tetraploidy is an intermediate state leading to chromosomal instability, aneuploidy, and tumorigenesis (Ganem *et al.*, 2007; Storchova and Kuffer, 2008). In animal and fungal cells, cytokinesis is achieved by a ring composed of filamentous actin (F-actin) and nonmuscle type II myosin (Satterwhite and Pollard, 1992; Fishkind and Wang, 1995). The actomyosin ring is a transient structure that is precisely positioned to bisect the elongating anaphase spindle, ensuring proper chromosome segregation (Pollard, 2010). In yeast, actomyosin ring contraction must be coordinated with septation, the process of adding new cell wall material between the dividing cells (Bi, 2001).

In budding yeast, both actomyosin ring assembly and contraction are cell cycle regulated. The type II myosin heavy chain, Myo1, forms a ring at the bud neck in G1 (Bi *et al.*, 1998; Lippincott and Li, 1998b). Localization of F-actin and contraction of the ring occur after anaphase and require the essential protein Iqg1/Cyk1 (Epp and Chant, 1997; Lippincott and Li, 1998b; Lippincott *et al.*, 2001). Iqg1 is a 173-kDa scaffolding protein homologous to mammalian IQGAPs. IQGAP family members are essential for actin-based processes such as phagocytosis, cell adhesion, migration, and cytokinesis (Shannon, 2012; White *et al.*, 2012). Iqg1 shares with other IQGAPs multiple functional domains: an N-terminal calponin homology domain (CHD), IQ repeats, a GTPase-related domain (GRD), and a Ras-GAP C-terminus (RGCt; Epp and Chant, 1997; Lippincott and Li, 1998a; Shannon, 2012). Iqg1 is recruited to the bud neck by

This article was published online ahead of print in MBoC in Press (http://www.molbiolcell.org/cgi/doi/10.1091/mbc.E14-12-1637) on June 17, 2015.

Address correspondence to: Katie B. Shannon (shannonk@mst.edu).

Abbreviations used: Cdk, cyclin-dependent kinase; CHD, calponin homology domain; FEAR, fourteen early anaphase release; MEN, mitotic exit network.

Supplemental Material can be found at:
http://www.molbiolcell.org/content/suppl/2015/06/14/mbc.E14-12-1637v1.DC1.html

the myosin regulatory light chain, Mlc1, via interactions with the IQ domains (Boyne *et al.*, 2000; Shannon and Li, 2000). Iqg1 recruitment to the ring is restricted to mitosis even though Mlc1 localizes to the bud neck earlier in the cell cycle (Boyne *et al.*, 2000; Shannon and Li, 2000). Iqg1 binds F-actin via the CHD and recruits F-actin to the bud neck during anaphase/telophase of mitosis, which completes actomyosin ring assembly (Shannon and Li, 1999). The C-terminus of Iqg1, containing both the GRD and RGCt domains, interacts with the GTPase Tem1 and is required for contraction of the actomyosin ring (Shannon and Li, 1999). Tem1 is part of the mitotic exit network (MEN), and temperature-sensitive alleles of Tem1 and other MEN proteins cause mitotic arrest in late anaphase before cytokinesis (Jaspersen *et al.*, 1998; McCollum and Gould, 2001).

The MEN, a signaling cascade that leads to the full release and activity of the phosphatase Cdc14, regulates mitotic exit, cytokinesis, and septation in budding yeast (Bardin and Amon, 2001; Meitinger *et al.*, 2012). The MEN brings about exit from mitosis by inactivating the mitotic cyclin-dependent kinase 1 (Cdk1). Cdk1, or Cdc28-Clb2 in budding yeast, is inactivated during anaphase via two partially redundant methods: inhibition of its kinase activity by Sic1 and degradation of the mitotic cyclin Clb2 by the APC^{Cdh1} complex (Jaspersen *et al.*, 1998; Visintin *et al.*, 1998). Both Sic1 and Cdh1 become active once dephosphorylated by the MEN component Cdc14, leading to inhibition of Cdk1 activity (Visintin *et al.*, 1998). When Cdk1 activity drops, MEN proteins Cdc15, Dbf2-Mob1, Dbf20-Mob1, and Cdc14 all accumulate to the bud neck by an unknown mechanism, where they are positioned to regulate cytokinesis and septation (Bembenek *et al.*, 2005; Meitinger *et al.*, 2012). Although Cdk1 must be inactivated in order for actomyosin ring assembly and contraction to occur, the MEN has a role in promoting cytokinesis in addition to Cdk1 inactivation (Meitinger *et al.*, 2012; Sanchez-Diaz *et al.*, 2012). Overexpression of *SIC1* bypasses mitotic arrest in most MEN mutants, but cytokinesis defects persist. In cells expressing temperature-sensitive alleles of the MEN gene *MOB1* and overexpressing *SIC1*, the actomyosin ring could assemble but not contract (Luca *et al.*, 2001). Similarly, inducing Cdc14 release after Tem1 depletion led to formation of actin rings that did not contract (Lippincott *et al.*, 2001), suggesting that the MEN regulates the timing of cytokinesis onset. Cdc14 can dephosphorylate the actin filament–nucleating formins Bni1 and Bnr1, which may affect the localization of the formins during cytokinesis, but whether this dephosphorylation affects actin ring assembly has not been shown (Bloom *et al.*, 2011). Cdc14 and the MEN kinase Dbf2 also play a role in septum regulation by targeting the chitin synthase Chs2. Cdc14 dephosphorylates Chs2 during anaphase, allowing Chs2 to localize to the bud neck, whereas Dbf2 phosphorylates Chs2 during actomyosin ring contraction, causing its dissociation from the bud neck (Chin *et al.*, 2012; Meitinger *et al.*, 2010; Oh *et al.*, 2012). Inn1 is another target of Cdc14, and dephosphorylation of Inn1 by Cdc14 also helps to regulate septation either through association of Inn1 with Cyk3 or via activation of Chs2 (Palani *et al.*, 2012; Kuilman *et al.*, 2015). Taken together, the results show that MEN has multiple targets that allow cell cycle coordination of mitotic exit, cytokinesis, and septation.

Because Cdc14 is the most downstream protein in the MEN pathway, the regulation of Cdc14 activity is key in coordination of cell cycle events. Early in the cell cycle, Cdc14 is bound to Net1, which inactivates and sequesters it in the nucleolus (Shou *et al.*, 1999; Visintin *et al.*, 1999). Two distinct mechanisms then release it from the nucleolus in an active form during anaphase. The Cdc14 early anaphase release network (fourteen early anaphase release [FEAR]) first releases Cdc14 into the nucleoplasm at anaphase onset primarily to promote proper spindle function and chromosome segregation. After chromosome segregation is completed, the MEN triggers widespread release of Cdc14 to the cytoplasm (Queralt and Uhlmann, 2008; Uhlmann *et al.*, 2011). Although many Cdc14 target proteins required for mitotic exit and other mitotic events are well characterized, a direct role for Cdc14 in regulating actomyosin ring assembly has not previously been described.

In the yeast *Candida albicans,* the Igq1 homologue is phosphorylated in vitro by the cyclin-dependent kinase Cdk1. Mutation of 15 minimal Cdk1 consensus sites (S/T-P) in Iqg1 flanking the CHD resulted in premature assembly and delayed disassembly of the actomyosin ring, resulting in cytokinesis defects (Li *et al.*, 2008). Budding yeast Iqg1 is phosphorylated in vivo by Cdk1 (Holt *et al.*, 2009), and a recent report demonstrated that loss of various combinations of N-terminal Cdk1 sites caused premature recruitment of Iqg1 and actin filaments to the contractile ring (Naylor and Morgan, 2014). Although there are 20 minimal consensus Cdk sites (S/T-P) in budding yeast Iqg1, only 4 match the strict Cdk consensus motif S/T-P-x-R/K, and these are all adjacent to the CHD near the Iqg1 N-terminus. Recently, Cdc14 was shown to possess specificity for the phosphoserine subset of the perfect Cdk consensus sites, and 3 of the CHD-flanking Cdk consensus sites also match the consensus for dephosphorylation by Cdc14 (Bremmer *et al.*, 2012; Eissler *et al.*, 2014). We hypothesized that dephosphorylation of these Cdk sites by Cdc14 is important for controlling Iqg1 function in cytokinesis. In this study we present genetic, cell biological, and biochemical evidence supporting this hypothesis and demonstrate that dephosphorylation of Iqg1 by Cdc14 is required for normal assembly of Iqg1 and F-actin in the contractile ring, providing insight into the mechanism of temporal regulation of cytokinesis.

RESULTS

Effects of Iqg1 phosphorylation mutations on cytokinesis

To test the hypothesis that the phosphorylation state of Iqg1 during the cell cycle is important for regulation of cytokinesis, we constructed two plasmids containing mutations of the four perfect consensus Cdk sites (S/TPxR/K, where x is any amino acid; Li *et al.*, 2008) that flank the CHD (Figure 1A). Using site-directed PCR mutagenesis, we mutated each serine or threonine to either alanine or glutamic acid. Two alleles were generated—*iqg1-4A*, with all four perfect Cdk sites mutated to alanine to prevent phosphorylation, and *iqg1-4E*, with all four amino acids mutated to glutamic acid to mimic phosphorylation. Both alleles were expressed using the endogenous *IQG1* promoter and tagged at the 3′ end with 13 copies of the myc epitope. Because it was uncertain whether cells expressing only the mutant alleles would be viable, each plasmid was introduced into a yeast strain that contains the wild-type copy of *IQG1* under the inducible *GAL1* promoter. This allowed the cells to be grown while expressing the wild-type copy of *IQG1* and for the wild-type copy to be repressed in order to see the effects of the mutations expressed using *IQG1* native promoter. As we have previously shown, the *GAL1-IQG1* is repressed after growth in yeast extract/peptone/dextrose (YPD) and phenocopies the null *IQG1* allele (Figure 1C, lane 3; Lippincott and Li, 1998b; Shannon and Li, 1999). Both mutant proteins were expressed at levels comparable to a similarly tagged wild-type Iqg1 protein (Figure 1C).

Cytokinesis defects in budding yeast cause a distinct phenotype in which cells continue to divide and rebud despite failing to separate, producing chains of cells (Figure 1D). To determine whether mutation of the Cdk phosphorylation sites affected cytokinesis, we examined the morphology of cells expressing the *iqg1-4A* and

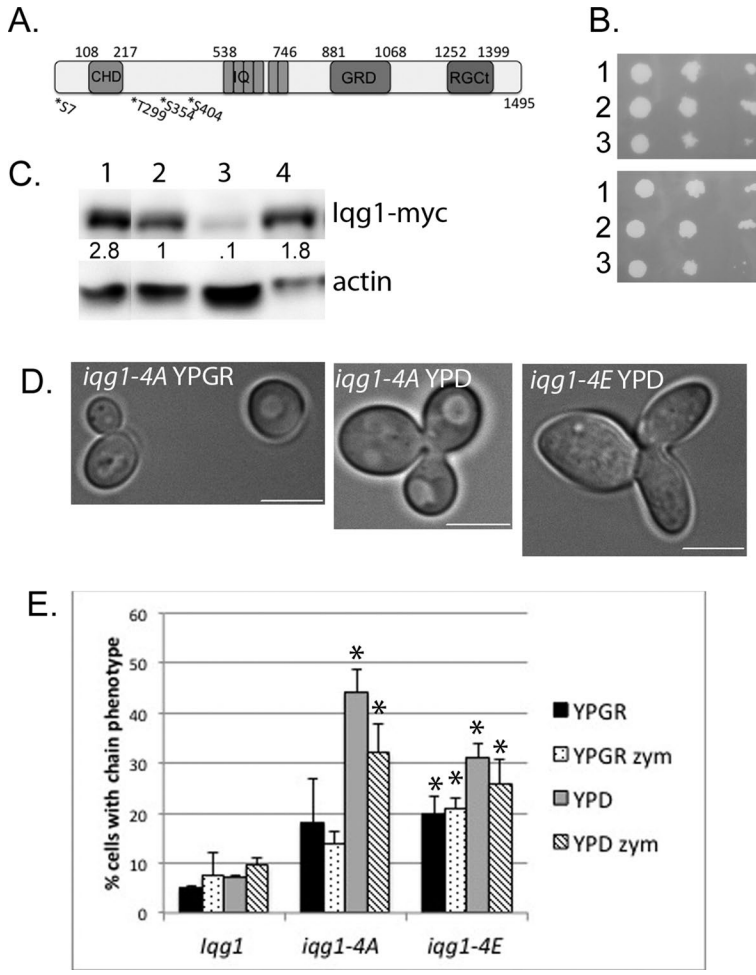

FIGURE 1: Effect of Iqg1 phosphorylation mutants on cytokinesis. (A) Schematic showing domains of Iqg1 to scale and the relative positions of the four perfect Cdk consensus sites. Domains in Iqg1 are the calponin homology domain (CHD), IQ motifs (IQ), GAP-related domain (GRD), and Ras GAP C-terminus (RGCt). Numbers above show the amino acids at the beginning and end of each domain; numbers below with asterisks represent the location of the four perfect Cdk consensus sites. (B) Cells were diluted, spotted on –His plates with galactose and raffinose (GR) or dextrose (D), and grown for 3 d at 30°C. Row 1, *IQG1-myc GAL1-IQG1*; row 2, *iqg1-4A-myc GAL1-IQG1*; row 3 *iqg1-4E-myc GAL1-IQG1*. (C) Western blot of cell extracts probed for Iqg1-myc and actin. Extracts were made from cells arrested in α factor in YPD for 3 h, followed by growth in YPD for 1 h to repress *GAL1-IQG1*. Lanes 1–4 are from the same Western blot, with an intervening lane between 1 and 2 cropped out. Lane 1, *iqg1-4A-myc GAL1-IQG1*; lane 2, *IQG1-myc GAL1-IQG1*; lane 3, *GAL1-IQG1*; lane 4, *iqg1-4E-myc GAL1-IQG1*. Numbers below Iqg1-myc bands are the Iqg1-myc band intensity adjusted for actin and normalized to wild type (lane 2). (D) Left, normal cell morphology of *iqg1-4A GAL1-IQG1* cells grown in YPGR. Middle, chain phenotype of three attached cell bodies of *iqg1-4A GAL1-IQG1* cells grown in YPD. Right, chain formed in *iqg1-4E GAL1-IQG1* cells in YPD. Scale bar, 5 μm. (E) Quantitation of chain phenotype. Cells containing wild-type *IQG1* under the *GAL1* promoter and either wild-type *IQG1* or phosphorylation mutant *iqg1-4A* or *iqg1-4E* expressed under the *IQG1* promoter were grown in YPGR (*GAL1-IQG1* expressed) or YPD (*GAL1-IQG1* repressed). For each replicate, 200 cells of each strain and treatment were counted and scored as chains if they contained three or more connected cell bodies. Zym indicates treatment with Zymolyase before microscopic examination. Error bars are SDs, and *p* values were calculated using the Student's *t* test in Excel (Microsoft, Redmond, WA) comparing *iqg1-4A GAL1-IQG1* and *iqg1-4E GAL1-IQG1* to *IQG1 GAL1-IQG1* cells under the same conditions. $*p \leq 0.01$.

iqg1-4E alleles. For comparison, the wild-type copy of *IQG1* under the *IQG1* promoter was also introduced into the strain with the wild-type copy of *IQG1* under the inducible *GAL1* promoter. The three strains—*IQG1 GAL1-IQG1*, *iqg1-4A GAL1-IQG1*, and *iqg1-4E GAL1-IQG1*—were grown in yeast extract/peptone/galactose/raffinose (YPGR) to allow wild-type *IQG1* expression from the *GAL1* promoter or YPD to repress *GAL1-IQG1* for 5–7 h before analysis. We previously showed that growth of the parental *GAL1-IQG1* strain in YPD represses expression of *IQG1* (Lippincott and Li, 1998b; Shannon and Li, 1999). Two hundred cells per treatment group were analyzed using light microscopy, and cells were scored as having the chain phenotype if they possessed three or more cell bodies (Figure 1, D and E). Control cells expressing *IQG1* from the endogenous promoter showed <10% of chained cells in all conditions (Figure 1E). Cells expressing *iqg1-4A* and wild-type *IQG1* from the *GAL1* promoter did not differ significantly from control cells in YPGR, indicating that *iqg1-4A* does not have a dominant-negative effect (Figure 1E). The cells expressing *iqg1-4A* exhibited altered morphology when wild-type *GAL1-IQG1* was repressed in YPD, forming chains in 44% of cells, significantly different both from controls expressing wild-type *IQG1* from the endogenous promoter and cells expressing both *iqg1-4A* and wild-type *IQG1* from the *GAL1* promoter ($p = 0.0002$ and 0.018; Figure 1E). Because yeast cells have a cell wall, it is possible that this chain phenotype is caused by defects in either septation or cytokinesis. To distinguish between the two possibilities, we used Zymolyase to remove the cell wall (Lippincott and Li, 1998b). After Zymolyase treatment, cells expressing only *iqg1-4A* still exhibited chains with significantly higher frequency than controls (32% compared with 9.5% in *IQG1* alone, $p = 0.002$, and 14% in *iqg1-4A GAL1-IQG1*–expressing cells, $p = 0.02$; Figure 1E).

In the strain expressing *iqg1-4E*, defects in cytokinesis were high both in the presence and absence of wild-type *IQG1* expressed from the *GAL1* promoter and with and without Zymolyase (Figure 1, D and E). In all cases, the percentage of chains in *iqg1-4E* cells was significantly higher than in control *IQG1* cells under the same conditions ($p \leq 0.01$). In addition to the high number of chains, the cell bodies in the chains were often elongated and appeared to be hyperpolarized (Figure 1D, right). *Iqg1-4E*, but not *iqg1-4A*, caused slower growth and smaller colonies on both plates with dextrose and plates with galactose and raffinose (Figure 1B). The reason for this is unknown, but it is possible that *iqg1-4E* is acting as a dominant negative, and therefore we did not further investigate the *iqg1-4E* allele.

Our results show that the *iqg1-4A* and *iqg1-4E* alleles affecting phosphorylation of Iqg1 cause a chain phenotype significantly above that of *IQG1* control cells. Because the *IQG1* mutant alleles

were expressed from a plasmid rather than the endogenous locus, we integrated a copy of *iqg1-4A* into the chromosome as described in *Materials and Methods*. The cells with integrated *iqg1-4A* had a significantly higher percentage of chains than the parental strain (11% in control cells compared with 24% in *iqg1-4A*; $p = 0.01$; Supplemental Figure S1). Our results are similar to those found in *Candida albicans*, demonstrating that the regulation of cytokinesis by phosphorylation of IQG1 is conserved between these yeast species. These data demonstrate that mutation of the four perfect Cdk sites in Iqg1compromises the cell's ability to complete cytokinesis.

Mutations that prevent phosphorylation of the Iqg1 Cdk sites cause actin ring formation before anaphase

In the yeast *C. albicans*, mutation of 15 minimal Cdk1 consensus sites in Iqg1 to alanine resulted in premature assembly of the actomyosin ring and cytokinesis defects (Li *et al.*, 2008). It was also recently reported that mutation of 14 Cdk sites in budding yeast Iqg1 caused actin ring formation before anaphase (Naylor and Morgan, 2014). We tested specifically whether the four perfect Cdk sites in Iqg1 flanking the actin-binding CHD domain were important for controlling the timing of actin recruitment to the ring. To do this, we examined the timing of actin ring formation in synchronous cell cultures. Assembly of the actomyosin ring is regulated during the cell cycle, with Iqg1 and F-actin localizing to the bud neck during anaphase (Lippincott and Li, 1998b; Lippincott *et al.*, 2001). Cells were arrested in G1 using mating factor. After release from the G1 arrest, a time course was performed with a sample of cells fixed every 20 min up to 100 min. The cells were stained using antibodies, phalloidin, and 4′,6-diamidino-2-phenylindole (DAPI) to visualize Iqg1, F-actin, and DNA, respectively. Images of >100 cells were analyzed at each time point under each condition in triplicate for the presence of actin and Iqg1 rings (Figure 2). Experimental cells were cultured in YPD to represses wild-type *GAL1-IQG1*, leaving *iqg1-4A* as the sole source of Iqg1 (Shannon and Li, 1999). Cells expressing only *iqg1-4A* were compared with cells expressing *iqg1-4A* and *GAL1-IQG1* (the same strain grown in YPGR), as well as to control cells with *IQG1* under the endogenous promoter in YPD.

In cells expressing only *iqg1-4A* (*iqg1-4A GAL1-IQG1* cells grown in YPD, henceforth referred to as *iqg1-4A* cells), formation of the actin ring occurred 20 min earlier in the time course than in both sets of control cells (Figure 2A). Approximately 13% of *iqg1-4A* cells had both an Iqg1 ring and an actin ring 40 min after release from arrest, whereas the same cells in YPGR had <1% at this time point, and cells expressing only *IQG1* had no rings at 40 min ($p = 9.2 \times 10^{-6}$ and 4.5×10^{-6}; Figure 2, A and B). The *iqg1-4A* cells that formed Iqg1 and actin rings at 40 min had not yet entered anaphase, indicated by the single DNA mass (Figure 2B). It is noteworthy that, contrary to a previous report, overexpression of wild-type *GAL1-IQG1* in YPGR control cells did not induce premature ring formation (Epp and Chant, 1997). At the 60- min time point, *iqg1-4A* and control cells contained actin rings. Control cells with both an Iqg1 ring and an actin ring either contained two DNA masses (Figure 2C) or an elongated mass of DNA spanning the bud neck, indicating that the cell is in anaphase. In *iqg1-4A* cells that had formed Iqg1 and actin rings at 60 min, some cells had yet to go through anaphase, since they had only a single nucleus (Figure 2, C and D). There was a significant increase in rings observed in *iqg1-4A* cells at the 60-min time point compared with controls, likely due to the fact that rings in *iqg1-4A* cells could be formed before anaphase, whereas in control cells, only those that had initiated anaphase contained rings ($p = 0.01$ compared with YPGR control and $p = 9.5 \times 10^{-6}$ compared with YPD control; Figure 2A). At the 20-min time point, no Iqg1 or actin rings were seen in control or experimental cells. At the 80- and 100-min time points, there was no statistically significant difference in the number of cells with Iqg1 and actin rings between the *iqg1-4A* cells and YPGR controls, but these cells did have a greater amount of rings than YPD controls (Figure 2A). These data show that expression of *iqg1-4A* at endogenous levels increased ring formation similar to overexpression of *IQG1* using the *GAL1* promoter, showing that *iqg1-4A* is constitutively active for actin ring formation. Overexpression of wild-type *IQG1* increases the number of rings relative to YPD controls but does not change the timing of ring assembly.

To analyze whether the Iqg1/actin rings formed before anaphase onset, we scored the DNA content of >100 *iqg1-4A* cells and YPD and YPGR control cells with rings at the 40-, 60-, and 80-min time points to determine whether there was one nucleus, two nuclei, or a nucleus in the process of division. Cells were judged to be in the process of division if the DAPI signal was elongated across the bud neck. Of Iqg1 and actin rings formed in control cells, 92–98% had a nucleus in the process of division or completely separated, indicating that actomyosin ring formation occurred after anaphase onset (Figure 2D). In contrast, 55% of *iqg1-4A* cells with rings had only a single nucleus, indicating that preventing phosphorylation of Iqg1 accelerated actin ring formation (Figure 2D). These results are consistent with the finding that wild-type cells form actin rings only when there is an anaphase spindle, whereas Iqg1 phosphomutants formed actin rings in cells with both preanaphase and anaphase spindles (Naylor and Morgan, 2014). Our data support the hypothesis that phosphorylation of the four perfect Cdk sites flanking the CHD of Iqg1 negatively regulates actin ring formation.

Changing Cdc14 levels affect actomyosin ring formation

Cdc14 is the final protein in the MEN signaling cascade and has been shown to dephosphorylate Cdk1 targets (Chin *et al.*, 2012; Visintin *et al.*, 1998). To test the hypothesis that Cdc14 regulates the timing of actin ring formation, we overexpressed *CDC14* in metaphase cells and examined formation of the actin ring. For these experiments, we obtained the *GAL1-CDC14* construct used by Sanchez-Diaz *et al.* (2012). Cells were arrested using the microtubule disruptor nocodazole, which activates the spindle assembly checkpoint and arrests cells before anaphase. Cells that had been cultured in YPD overnight were resuspended into YPD (control, *GAL1-CDC14* repressed) or YPGR (experimental, *GAL1-CDC14* expressed) simultaneously with nocodazole (5 μg/ml) and incubated for 2.5 h. Cells were analyzed for actin rings using A568 phalloidin. Cells overexpressing *CDC14* formed twice as many actin rings as control cells ($p = 0.008$; Figure 3, A and B). The increase in actin rings in nocodazole-arrested cells overexpressing *CDC14* indicates that Cdc14 activity can promote premature actin ring formation. Control cells exhibited a higher percentage of actin rings than expected, since wild-type cells do not form actin rings in nocodazole (Naylor and Morgan, 2014), but this may be due to incomplete inhibition of the *GAL1* promoter in YPD and elevated Cdc14 protein levels. It was reported that overexpression of Cdc14 improves the efficiency of cytokinesis when Cdk is inactivated before anaphase (Sanchez-Diaz *et al.*, 2012).

If Cdc14 regulates the timing of actin ring formation by reversing inhibitory phosphorylation by Cdk1, then *cdc14-1* mutants will be defective for actin ring formation. Although actin ring formation has been seen in many MEN mutants after bypassing mitotic arrest, a careful analysis of actin ring formation in *CDC14* mutant cells has not been reported. To determine whether actin ring formation requires Cdc14 function, we used a temperature-sensitive mutant

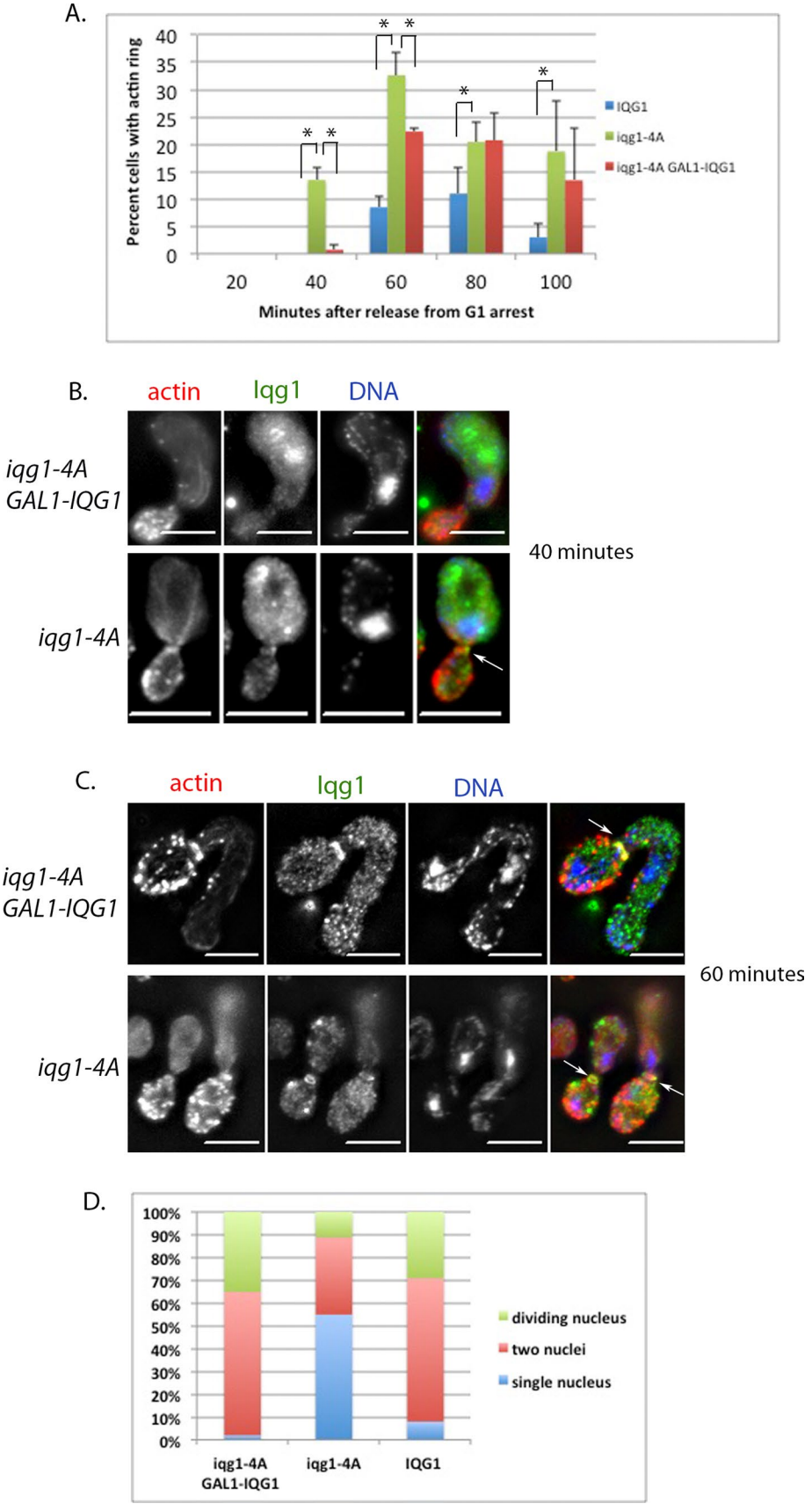

FIGURE 2: Mutations preventing phosphorylation of Iqg1 lead to formation of the actin ring before anaphase. (A) Timing of actin ring formation. Cells were synchronized in G1 using α factor, and time points were taken at 20-min intervals after release from arrest. During α factor arrest, *IQG1 GAL1-IQG1* or *iqg1-4A GAL1-IQG1* cells were cultured in medium containing galactose (YPGR) to allow expression of wild-type *GAL1-IQG1* or glucose (YPD) to repress expression of *GAL1-IQG1*. Labels in the key show which genes were expressed. Average of three experiments with 100 cells analyzed at each time point. Error bars are SDs, and *p* values were calculated using the Student's *t* test in Excel. $*p \leq 0.01$
(B) Examples of cells at 40 min. Actin, Iqg1, and DNA in *iqg1-4 GAL1-IQG1* cells grown in YPGR as a control (top) and *iqg1-4A GAL1-IQG1* experimental cells grown in YPD (bottom) at the 40-min time point.
(C) Examples of cells with actin and Iqg1 rings at 60 min. Control *iqg1-4 GAL1-IQG1* cells in YPGR (top) and *iqg1-4A GAL1-IQG1* experimental cells grown in YPD (bottom) at the 60-min time point. For B and C, labels on the left show which genes were expressed. Images are deconvolved single-plane projections of a *Z*-series. Scale bar, 5 μm. Arrows in merged panels show actin and Iqg1 rings. (D) *IQG1 GAL1-IQG1* or *iqg1-4 GAL1-IQG1* cells containing actin and Iqg1 rings were examined using DAPI staining to determine whether they contained one nucleus, two nuclei, or a nucleus in the process of dividing. The *x*-axis is labeled to reflect the genes expressed: IQG1 is *IQG1 GAL1-IQG1* cells grown in YPD, iqg1-4A is *iqg1-4 GAL1-IQG1*cells grown in YPD, and iqg1-4A GAL1-IQG1 is *iqg1-4 GAL1-IQG1*cells grown in YPGR.

allele of *CDC14*, *cdc14-1*, and bypassed mitotic arrest using a 2μ plasmid containing *SIC1*. Cells were cultured overnight and synchronized in mitosis using nocodazole for 90 min at room temperature. Next they were incubated at room temperature (control) or 37°C (experimental) to inhibit *cdc14-1* activity, for an additional 90 min. Samples were taken during nocodazole arrest, and then the nocodazole was removed, and two time points were taken after release from mitotic arrest. Cells were fixed, stained for actin, and examined by epifluorescence microscopy.

In nocodazole, *cdc14-1* cells almost completely failed to form actin rings at the nonpermissive temperature (2% of cells; $p = 0.001$; Figure 3C). In the room temperature controls, ~18% of cells formed rings due to the overexpression of *SIC1*, as previously reported (Sanchez-Diaz *et al.*, 2012). After release from mitotic arrest, actin ring formation in *cdc14-1* cells remained significantly higher in room temperature controls than in the nonpermissive experimental conditions at both 10- and 20-min time points (Figure 3C). These data show that Cdc14 activity is important for actin ring formation in addition to its role in inactivating Cdk1.

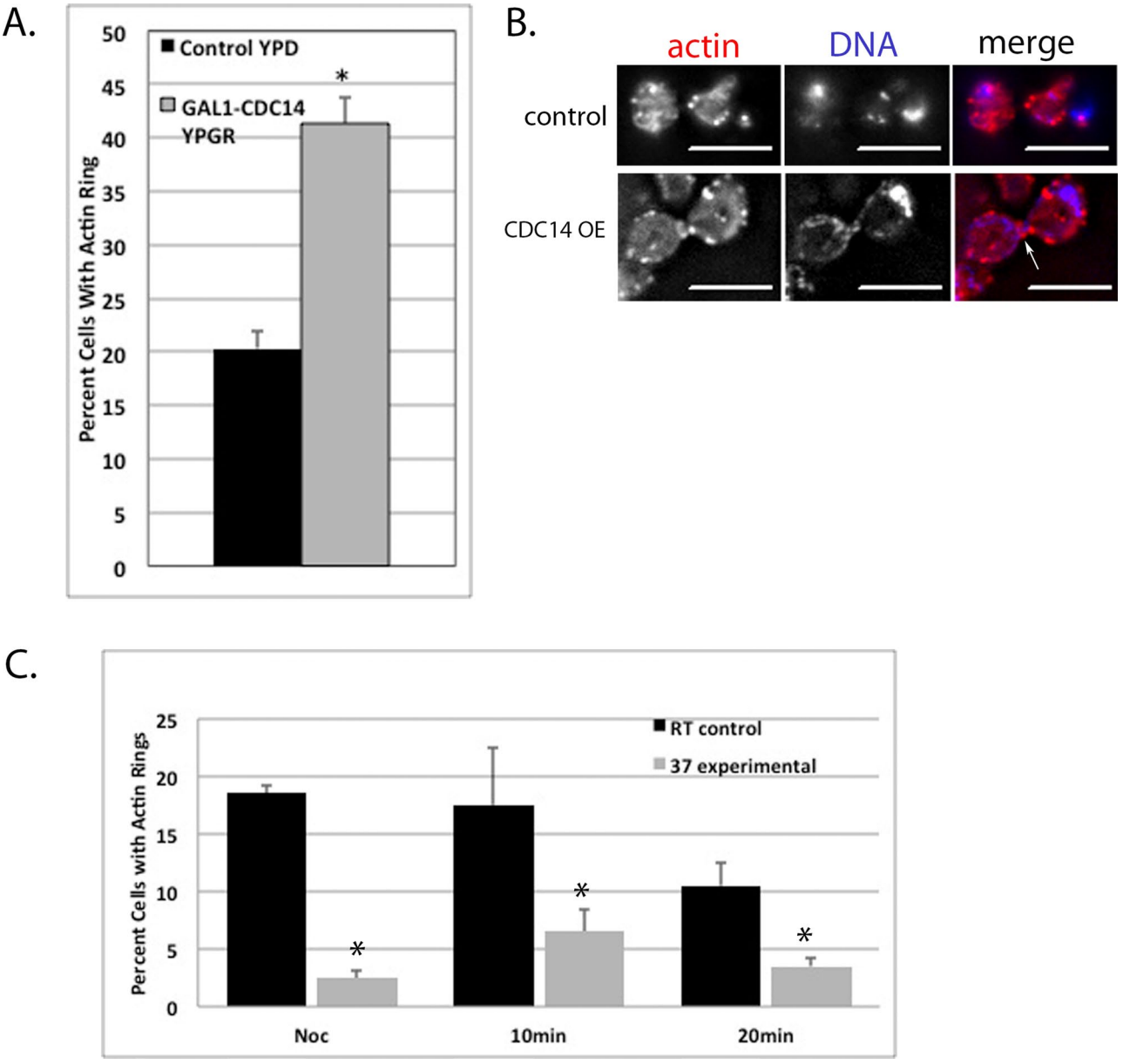

FIGURE 3: Cdc14 regulates actin ring formation. (A) Overexpression of Cdc14 causes formation of actin rings during mitotic arrest. Cells containing *CDC14* under the *GAL1* promoter were used to selectively overexpress Cdc14. Cells grown in glucose were pelleted and resuspended in medium with nocodazole containing either glucose (control) or galactose (experimental) for 2.5 h at 30°C and then fixed for imaging. Actin rings were quantified in three replicates of 100 cells/treatment type. Data are the averages with SDs. A *p* value of 0.008 was obtained using the Student's *t* test. (B) Actin and DNA staining during nocodazole arrest. Top, lack of actin ring in control cell (YPD); bottom, actin ring formation in *GAL1-CDC14* cells. Arrow indicates actin ring. Scale bar, 5 μm. (C) Effect of inhibiting Cdc14 activity on actin ring formation. Cells with a temperature-sensitive *cdc14-1* allele and *SIC1* expressed from a 2μ plasmid were diluted into YPD with addition of nocodazole for 90 min to arrest cells in mitosis. Cells were then placed at room temperature or 37°C for 90 min and fixed during and after release from nocodazole arrest. Noc, cells in nocodazole; 10 and 20 min are minutes after release from nocodazole arrest. Actin rings were quantified in three replicates of 100 cells/treatment type. Data are the averages with SDs. $*p \leq 0.05$.

The failure of *CDC14* mutants to form actin rings can be rescued by expression of *iqg1-4A*

Because *iqg1-4A* and overexpression of *CDC14* affect the timing of actin ring formation, and *cdc14-1* cells overexpressing *SIC1* fail to form actin rings at the nonpermissive temperature, Cdc14 might regulate actin ring formation through dephosphorylation of Iqg1 at Cdk sites. To test this hypothesis, we used control cells that contained *cdc14-1* and *GAL-SIC1ΔNT-myc* to bypass mitotic arrest (Chin *et al.*, 2012). Experimental cells combined the *cdc14-1* and *GAL-SIC1ΔNT-myc* alleles with *iqg1-4A* and a chromosomal deletion of wild-type *IQG1*, leaving *iqg1-4A* as the sole source of Iqg1.

Cells were synchronized in mitosis using nocodazole for 90 min at room temperature and then resuspended in YPGR (to overexpress *SIC1*) with nocodazole and incubated at 37°C to inhibit

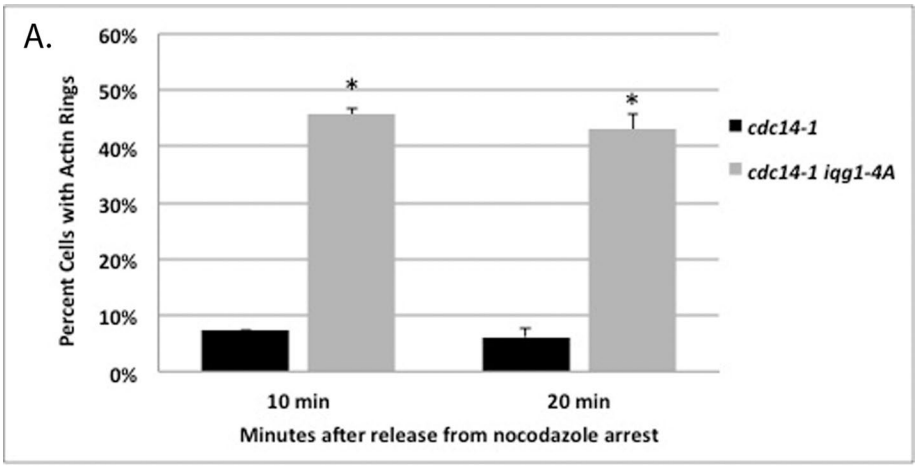

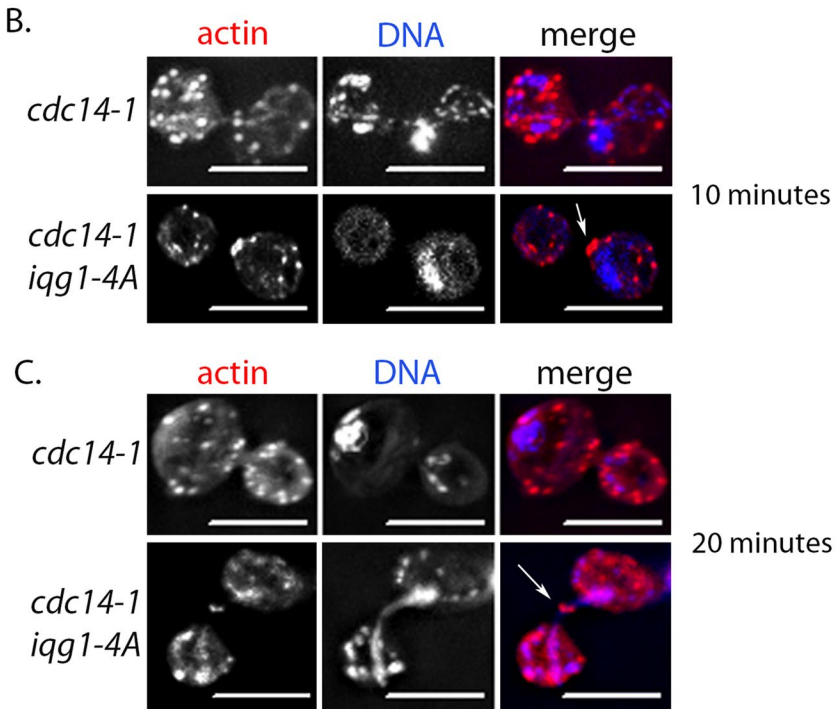

FIGURE 4: The Iqg1 phosphomutant rescues actin ring formation in *cdc14-1*cells. Control cells in this experiment were of the genotype *cdc14-1 GAL1-SIC1ΔNT*, and the experimental cells were *cdc14-1 GAL1-SIC1ΔNT iqg1-4AΔIQG1*. Cells were grown overnight in medium containing glucose at room temperature and then resuspended in fresh medium with addition of nocodazole for 90 min to arrest in mitosis. Cells were then resuspended in YPGR (to overexpress *SIC1*) with nocodazole, incubated at 37°C for 90 min, and fixed after release from nocodazole at 10 and 20 min. (A) Actin staining was performed, and the percentage of cells containing an actin ring was determined after examining 100 cells for each strain at each time point. *$p < 0.01$ (10 min $p = 0.0003$; 20 min $p = 0.001$). (B, C) Single-plane projections of a deconvolved *Z* series of *cdc14-1* (top) and *cdc14-1 iqg1-4A* (bottom) cells stained with phalloidin and DAPI after release from nocodazole for either 10 min (B) or 20 min (C). Actin column shows phalloidin fluorescence, and DNA column is DAPI staining. Arrows point to actin rings. Scale bar, 5 μm.

cdc14-1 activity, for an additional 90 min. After release from nocodazole arrest, samples were taken at 10 and 20 min, fixed, and stained using phalloidin to visualize F-actin. Similar to the previous experiment, *cdc14-1 GAL-SIC1ΔNT-myc* control cells formed few actin rings at either time point (7 and 6%; Figure 4, A–C). However, for the *cdc14-1 GAL-SIC1ΔNT-myc iqg1-4A* strain, 46% of cells at the 10-min time point and 44% of cells at the 20-min time point contained actin rings ($p = 0.0003$ and 0.001; Figure 4A). The *cdc14-1 GAL-SIC1ΔNT-myc iqg1-4A* cells 10 min after release from metaphase arrest typically had a single DNA mass, indicating preanaphase cells (Figure 4B), whereas 20 min after release, some cells had segregated DNA (Figure 4C). The *iqg1-4A* mutant rescues the *cdc14-1* mutant allele's inability to assemble an actin ring. These results suggest that Iqg1 is the primary Cdc14 target involved in temporal regulation of actin ring formation.

Iqg1 and Cdc14 interact in vivo, and Iqg1 is a Cdc14 substrate in vitro

Because our experiments suggested that Iqg1 is the target of Cdc14 that regulates actin ring formation, we looked for an interaction between Iqg1 and a substrate trap Cdc14 mutant in yeast extracts by coimmunoprecipitation (coIP). Wild-type Iqg1 copurified with the Cdc14 substrate-trap protein (Figure 5A). However, an Iqg1 mutant (Iqg1-3T) in which the Cdk phosphorylation sites at positions 7, 354, and 404 were changed from serines to threonines did not copurify with the Cdc14 substrate trap. Cdc14 is highly selective for phosphoserines within consensus Cdk sequences (Bremmer *et al.*, 2012). This result suggests that Cdc14 recognizes Iqg1 as a substrate and that recognition is dependent on just three N-terminal Cdk sites that flank the CHD and contain the optimal Cdc14 recognition motif.

We also directly tested whether the N-terminal Cdk sites flanking the CHD could be efficiently dephosphorylated by Cdc14 in vitro, using phosphopeptide substrates. Cdc14 specificity can be effectively evaluated using phosphopeptides, and catalytic efficiency of Cdc14 toward phosphopeptides containing different Cdk phosphorylation-site sequences can vary by several orders of magnitude (Bremmer *et al.*, 2012). As expected, phosphorylated Ser-354 and Ser-404 peptides were very efficient substrates, comparable to a previously characterized optimal site in the Acm1 protein (Figure 5B). The peptide containing phosphorylated Thr-299 exhibited essentially no activity, consistent with Cdc14's selectivity for serine Cdk sites. Two additional Ser Cdk sites that lack the optimal Lys/Arg at position +3, pS365 and pS1347, were used as controls and were dephosphorylated at lower rates, as expected. Surprisingly, phosphorylated Ser-7 was not dephosphorylated as efficiently as Ser-354 and Ser-404, even though this serine is followed by a lysine at the +3 position (Figure 4B). Nonetheless, these data confirm that at least two of the four perfect Cdk sites near the Iqg1 N-terminal CHD behave as optimal Cdc14 substrate sites in vitro.

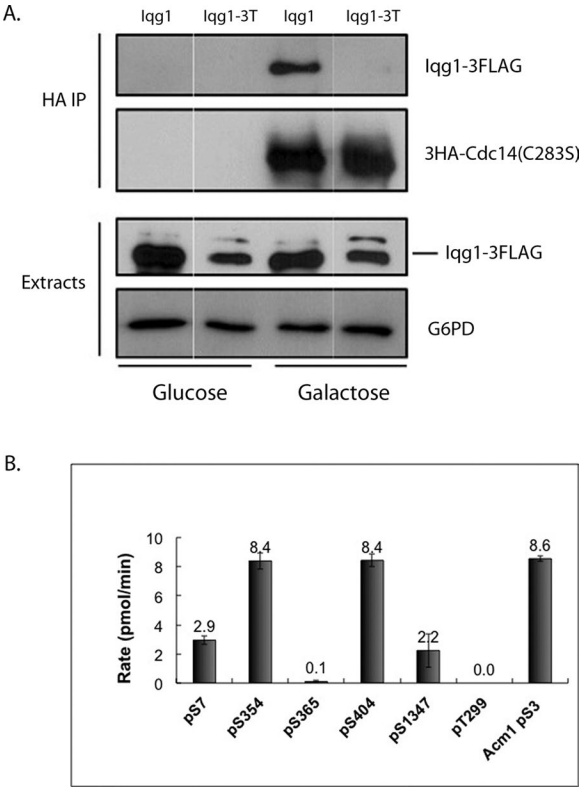

FIGURE 5: Iqg1 is recognized as a substrate by Cdc14 in vivo and in vitro. (A) CoIP of Iqg1 and a Cdc14 substrate trap mutant. 3HA-Cdc14(C283S) expressed from the *GAL1* promoter was isolated from soluble protein extracts on anti-HA affinity resin and the presence of associated Iqg1-3FLAG or Iqg1-3T-3FLAG monitored by immunoblotting. Glucose conditions that suppress the *GAL1* promoter were used as a negative control. Glucose-6-phosphate dehydrogenase is a loading control for the extract samples. (B) Dephosphorylation of phosphopeptides derived from Iqg1 by Cdc14. Synthetic phosphopeptides with phosphorylation sites at the indicated amino acid positions of Iqg1 or Acm1 were treated with purified recombinant Cdc14 under identical steady-state reaction conditions (substrate concentration, enzyme concentration, time) and the rate of dephosphorylation calculated. Under the conditions used, rate differences should reflect differences in catalytic efficiency (k_{cat}/K_m). Data are the average of three independent experiments, and error bars are SDs.

Actomyosin ring contraction defects in *iqg1-4A* cells

Because cells expressing *iqg1-4A* formed actin rings early and had cytokinesis defects, we used live-cell imaging to examine actomyosin ring contraction. We considered that actomyosin ring contraction might be occurring early, since the ring is assembled earlier, or that the rate or symmetry of contraction might be affected. For these experiments, we used cells expressing *iqg1-4A*, *MYO1–green fluorescent protein* (*GFP*), and *TUB1-mCherry* (Shannon and Li, 1999; Khmelinskii *et al.*, 2007). Contraction of the actomyosin ring did not occur earlier in the cell cycle in *iqg1-4A* cells, as Tub1-mCherry showed that the spindle was completely elongated before contraction began (Figure 6A). In control cells, Myo1-GFP exhibited symmetric contraction to a single dot over an average of 8.1 ± 1.0 min, consistent with previous results ($N = 6$; Figure 6B; see Supplemental Figure 6B.mov for another example; Lippincott and Li, 1998b; Bi, 2001; Stockstill *et al.*, 2013). However, Myo1-GFP failed to contract normally in *iqg1-4A* cells. Cells expressing *iqg1-4A* exhibited what appeared to be disassembly of Myo1-GFP, with the GFP signal becoming dimmer without the diameter of the ring decreasing ($N = 6$; Figure 6C; see Supplemental Figure 6C.mov for another example). This loss of Myo1-GFP signal occurred over the same length of time as contraction in control cells, 8.3 ± 2.2 min. To look at disassembly of Myo1-GFP, we generated a fluorescence intensity plot. In contrast to control cells, the Myo1-GFP signal rapidly decreased in intensity, without the peaks moving closer together as during contraction in control cells (Figure 6C). It was shown previously that preventing nuclear export of Cdc14 to the cytoplasm caused cytokinesis defects and a failure of Myo1-GFP to contract (Bembenek *et al.*, 2005). Therefore timely dephosphorylation of Cdc14 targets at the bud neck may be essential for normal myosin contraction. A defect in Myo1-GFP contraction was recently reported in cells in which the Cdc14 target Inn1 was forced to undergo constitutive Cdk phosphorylation (Kuilman *et al.*, 2015). Therefore there are at least two Cdc14 targets—Iqg1 and Inn1—required for proper contraction of myosin during cytokinesis.

The bud necks of the *iqg1-4A* cells were significantly larger than control cells, 1.9 compared with 1.3 µm ($p = 0.0002$). Effects on the size of the bud neck have been seen after perturbation of many other cytokinesis and septation genes, including Hof1, Cyk3, Inn1, and Chs2 (Lippincott and Li, 1998a; Korinek *et al.*, 2000; Stockstill *et al.*, 2013; Kuilman *et al.*, 2015). Mechanistically, the reason for the altered bud neck size is unknown, but it is likely due to the coupling between cytokinesis, septation, and selection of the future bud site in budding yeast. Our results suggest that timely phosphorylation and dephosphorylation of Iqg1 is needed to ensure normal contraction of the ring during cytokinesis and maintenance of normal bud neck morphology.

DISCUSSION

Dephosphorylation of Iqg1 by Cdc14 regulates actin ring assembly

Actin ring assembly in budding yeast is restricted to anaphase, but the mechanism by which this is accomplished has been unclear. Expression of Iqg1 is cell cycle regulated, and Epp and Chant (1997) reported that overexpression of Iqg1 was able to drive premature actin ring assembly. However, in our strain background, overexpression of *IQG1* using the *GAL1* promoter did not affect the timing of actin ring assembly. This can be seen from the data in Figure 2, where control cells cultured in YPGR that overexpress *IQG1* do not form actin rings before anaphase.

In *C. albicans*, phosphorylation of Iqg1 by Cdk1 at 15 perfect and minimal Cdk consensus sites was shown to affect the timing of actin ring formation (Li *et al.*, 2008). During the course of our study, it was shown that inhibition of Cdk1 activity in metaphase cells and Iqg1 mutations that prevent phosphorylation at N-terminal Cdk site clusters cause premature actin ring assembly in *Saccharomyces cerevisiae* (Naylor and Morgan, 2014). In that study, mutation of two distinct Cdk site clusters chosen based on proximity within the primary sequence resulted in partial actin ring assembly phenotypes, whereas a more severe effect on actin ring formation was observed with simultaneous mutation of both clusters, containing 14 perfect and imperfect Cdk sites total. This suggested that Iqg1 function in directing final actomyosin ring maturation is controlled by multiple Cdk phosphorylation events spread over a relatively large primary sequence space. A role for Cdc14, or another phosphatase, in the dephosphorylation and regulation of Iqg1 was not addressed in either of these studies. Here, we showed that 1) preventing phosphorylation of just the four perfect Cdk sites in the N-terminus of

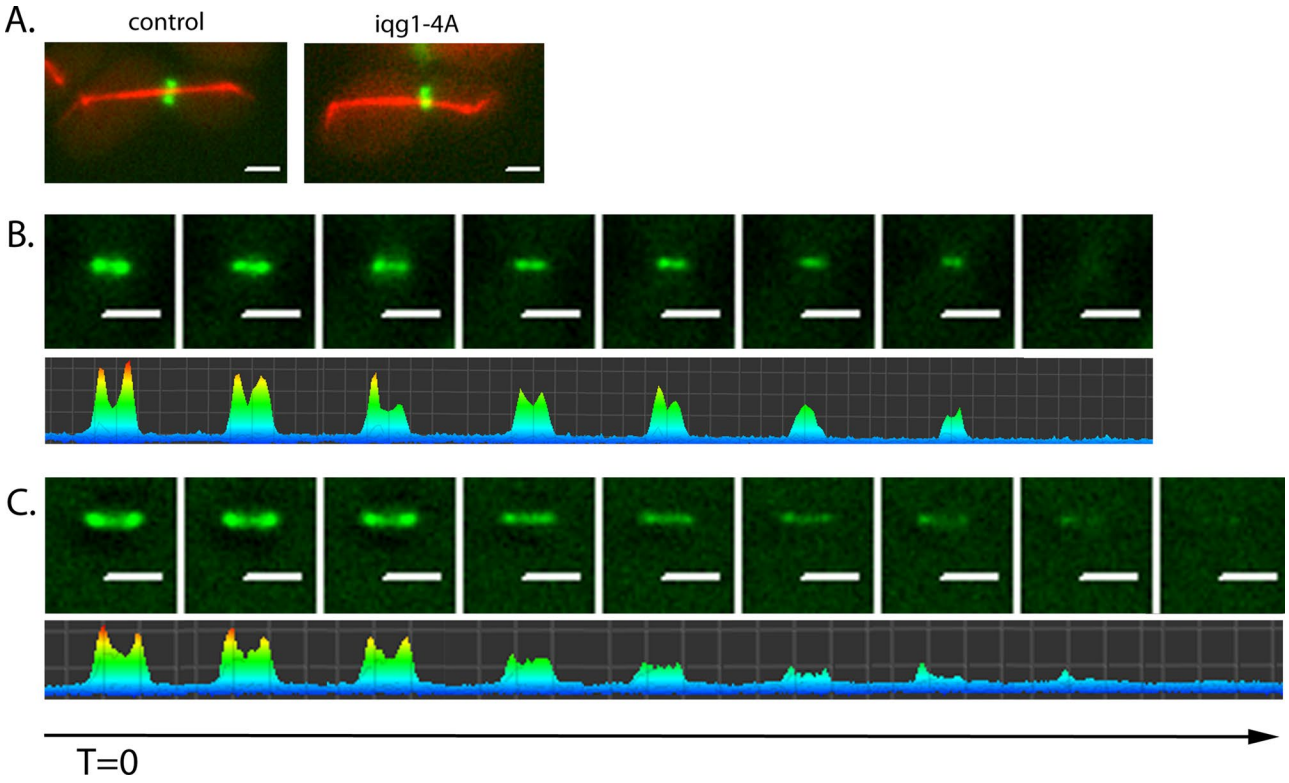

FIGURE 6: The actomyosin ring does not contract in *iqg1-4A* mutant cells. (A) Live-cell imaging was performed on cells expressing Myo1-GFP and Tub1-mCherry. Left, representative control cell; right, a typical *iqg1-4A* cell. All cells showed elongated spindles as shown before actomyosin ring contraction or disassembly occurred. (B) Live-cell imaging of a control cell showing contraction of the actomyosin ring. (C) Live-cell imaging of a *iqg1-4A* cell, showing that the actomyosin dissembles but does not contract. For both B and C, the top shows the Myo1-GFP signal and the bottom shows the two-dimensional fluorescence intensity of the signal. Scale bar, 2 μm. The panel on the left is $T = 0$, which is the time point before the beginning of either contraction or disassembly. Each panel represents an image taken at 1-min intervals.

Iqg1 (which come from both of the clusters analyzed by Naylor and Morgan, 2014) is sufficient to cause premature actin ring formation and 2) Iqg1 is a novel substrate of Cdc14 whose dephosphorylation at a few perfect Cdk sites helps to regulate the timing of actin ring assembly and the fidelity of actomyosin ring function.

Our results are largely consistent with the conclusions of Naylor and Morgan (2014). Both studies found that Cdk phosphorylation of sites in the Iqg1 N-terminus restrain actin ring formation until late anaphase after chromosome segregation is completed. Both studies likewise observed early recruitment of Iqg1 to the division site when Cdk phosphosites were mutated. Also consistent with their work, we did not observe premature contraction of Myo1 in cells expressing the *iqg1-4A* mutant, confirming their conclusion that actomyosin ring assembly and constriction are regulated independently. Our results differ from theirs in that they did not report cytokinesis phenotypes or Myo1 contraction defects in their Iqg1 phosphomutant cells, and the reason for this difference is unclear, since both studies were done in the W303 background and involved integrated *IQG1* alleles expressed under the endogenous promoter (Naylor and Morgan, 2014). However, our results are consistent with analysis of Iqg1 in *C. albicans*, where premature actin ring assembly correlated with cytokinesis defect and aberrant Myo1-GFP contraction (Li *et al.*, 2008).

Of the four amino acids mutated in our study, serines at 354 and 404 of Iqg1 have been shown to be phosphorylated by Cdk1/Cdc28 in a cell cycle–dependent manner in vivo (Holt *et al.*, 2009). We demonstrated that these two serines are Cdc14 substrates in vitro. Although phosphorylation of serine has not been observed at S7, this peptide may be poorly detected by MS. Serine 7 is predicted to be phosphorylated by the NetPhos2.0 neural network predictor of eukaryotic phosphorylation sites (Blom, 1999). This serine was not an effective Cdc14 substrate in vitro, so whether the phosphorylation and dephosphorylation of this residue occurs in vivo is unclear. Phosphorylation of the threonine at position 299 has also not been detected in vivo but is predicted to occur, although this threonine is not a Cdc14 substrate (Blom, 1999). Further studies are needed to determine whether the threonine at position 299 remains phosphorylated after the serines are dephosphorylated by Cdc14 and to define its functional importance.

Regulation of cytokinesis may be a conserved function of Cdc14 phosphatases. In addition to its requirement for cytokinesis in budding yeast, Cdc14 homologues have been reported to affect cytokinesis also in fission yeast, *Caenorhabditis elegans*, *Xenopus laevis*, and humans, although few molecular targets affecting cytokinesis have been identified in these systems (Mocciaro and Schiebel, 2010). In fission yeast, the Cdc14 homologue Clp1 localizes to the division site through binding to the anillin orthologue Mid1, where it stabilizes the contractile ring (Clifford *et al.*, 2008). One key substrate of Clp1 at the contractile ring is Cdc15, a Hof1 homologue and an important regulator of actomyosin ring assembly, function, and septation (Clifford *et al.*, 2008). The Iqg1 orthologue Rng2 may be another contractile ring substrate of Clp1, because it was identified as a Clp1 binding partner in a recent proteomics analysis, although the functional importance of the Clp1 interaction with Rng2 has not been demonstrated (Chen *et al.*, 2013). Overall, few targets of Cdc14 orthologues directly involved in execution of cytokinesis

are known. Our data reveal that Cdc14 functions in the final stage of actomyosin ring assembly in budding yeast and suggest that Iqg1 is the sole Cdc14 target that regulates the timing of actin ring assembly.

Role of the MEN in actomyosin ring assembly

In light of our results that Cdc14 function is needed for normal actin ring formation before cytokinesis, it is somewhat surprising that previous studies with conditional MEN mutants upstream of Cdc14 did not observe a similar defect (Vallen *et al.*, 2000; Lippincott *et al.*, 2001; Luca *et al.*, 2001). A critical function of the MEN in promoting cytokinesis is to release Cdc14 from nucleolar sequestration and target it to the cytoplasm, where it can dephosphorylate its cytokinetic targets (Bembenek *et al.*, 2005; Mohl *et al.*, 2009; Sanchez-Diaz *et al.*, 2012; Kuilman *et al.*, 2015). In the previous studies of the MEN proteins Tem1and Mob1, mitotic exit was induced by using either *net1-1* temperature-sensitive allele or *SIC1* overexpression, and it is likely that active Cdc14 was released from the nucleolus as a result (Luca and Winey, 1998; Lippincott *et al.*, 2001). In the case in which *dbf2-2* was examined at the semipermissive temperature or a *CDC15* deletion mutant was used and actin ring formation was normal, there may not be a complete absence of Cdc14 activity (Menssen *et al.*, 2001; Hwa Lim *et al.*, 2003). One prior study did report that actin rings form normally in *cdc14* cells (Vallen *et al.*, 2000). However, the results were based on single time points after a long incubation at restrictive temperature and therefore would not reveal the changes in the kinetics of ring formation that we report here.

It will be important to determine in future studies the activity and localization of Cdc14 relative to actomyosin ring formation and contraction. We are evaluating actin ring formation in FEAR network mutants to test whether FEAR-released Cdc14 can support actin ring formation.

Mechanism by which phosphorylation regulates Iqg1 function

Another question raised by our study is how the phosphorylation of Iqg1 by Cdk1 prevents actin ring assembly before anaphase. One attractive hypothesis is that phosphorylation of the Cdk sites alters the ability of Iqg1 to bind to F-actin, since the Cdk sites flank the CHD. Alternatively, rather than affect the binding to F-actin directly, the phosphorylation mutants could affect Iqg1's interactions with formin proteins Bni1 and Bnr1, as has been shown in *C. albicans* (Li *et al.*, 2008). Iqg1, Bni1, and Bnr1 are all required for actin ring assembly in budding yeast, but how they might cooperate in generating the actin ring is not known (Shannon and Li, 1999; Tolliday *et al.*, 2002). Phosphorylation of Iqg1 could also prevent interaction with other proteins, such as those that help recruit Iqg1 to the contractile ring. This would be consistent with the observation that the Iqg1-4A mutant protein appears earlier than the wild-type protein at the bud neck. The IQ domains of Iqg1 interact with Mlc1, and this interaction is important for recruiting Iqg1 to the contractile ring (Shannon and Li, 2000). The IQ domains are also situated in the Iqg1 N-terminal region just downstream of several of the optimal Cdc14 target sites (Figure 1A). However, the recent study by Naylor and Morgan (2014) did not find any evidence that Cdk site mutations affected the interaction between Iqg1 and Mlc1, and the interaction between *iqg1-4A* and *iqg1-4E* mutants and GST-Mlc1 in a GST pull-down assay was indistinguishable from wild-type Iqg1 (our unpublished data).

How mutation of the phosphorylation sites in Iqg1 causes cytokinesis defects is unclear. The interaction between Iqg1 and Tem1 is required for myosin ring contraction, but the GRD of Iqg1 that mediates the interaction with Tem1 is not near the Cdk sites (Shannon and Li, 1999). The mechanism by which the *iqg1-4A* mutant affects contraction of the actomyosin ring could be due to loss of coordination between cytokinesis and septation (Bi, 2001). Iqg1 is assumed to have a function in septation, since it is an essential gene, and cytokinesis is not an essential process in budding yeast, but exactly how Iqg1 might function to link septation and cytokinesis is unclear. One possibility is through an interaction with the Hof1 protein, which promotes primary septum deposition by Chs2 and is required for normal myosin contraction and bud neck size (Lippincott and Li, 1998a; Nishihama *et al.*, 2009). Iqg1 interacts with Hof1 directly, and Hof1 appeared at the bud neck prematurely in cells expressing Cdk1 phosphorylation-deficient Iqg1 (Naylor and Morgan, 2014; Tian *et al.*, 2014). Thus it is conceivable that the misregulated assembly of proteins in the contractile ring in the absence of normal Iqg1 phosphorylation results in a structurally and functionally compromised ring.

There are other possible mechanisms by which the Iqg1-4A mutant protein could perturb ring contraction. A quantitative model for generation of force in the actomyosin ring suggested that Iqg1 could augment cofilin function in the ring by acting as a cross-linker during actin filament depolymerizaiton (Mendes Pinto *et al.*, 2012). If mutation of the phosphorylation sites disrupts the ability of Iqg1 to act as an actin cross-linker during actomyosin ring contraction, it could result in lack of contraction seen. To test this hypothesis, the effect of mutations on Iqg1's cross-linking function and modeling studies will be needed.

Regardless of the mechanisms by which phosphorylation acts, a general conclusion of our work is that Cdc14 regulation of Iqg1 function contributes to the proper temporal coordination of cytokinesis after nuclear division is complete.

MATERIALS AND METHODS

Strains and media

All *S. cerevisiae* strains were derived from the W303 background and are listed in Table 1. Cultures were grown at 30°C in YEP + 2% D-glucose (YPD) or YEP + 2% galactose and raffinose (YPGR), except where noted.

Plasmid construction and mutagenesis

Plasmids are listed in Table 2. To make the *IQG1* phosphomutant plasmids, the QuikChange II XL Multi Site-Directed Mutagenesis Kit (Aligent Technologies, Santa Clara, CA) was used to mutate pTL12, which contains full-length *IQG1* under its endogenous promoter with a 13-myc tag on the C-terminus (Lippincott and Li, 1998b). The kit was used per manufacturer's instruction with a few modifications. The PCR primer amount was sensitive and needed to be 200 ng with template DNA concentration at 30 ng. The *Pfu* was added 5 min after starting the following program: 95°C for 6 min, 1 cycle, 98°C for 1 min, 55°C for 1 min, 65°C for 20 min, 18 cycles, 72°C for 7 min, 1 cycle.

Miniprep plasmid isolation on the Site-Directed Mutagenesis transformation colonies was performed according to the Wizard Plus SV Minipreps DNA Purification System (Promega, Madison, WI) protocol, and resulting purified DNA was sequenced by Missouri S&T cDNA Resource Center for verification of mutations. The four consensus Cdk sites are located at amino acids S7, T299, S345, and S404. All four sites were changed either to alanine or to glutamic acid, creating two final plasmids, expressing *igq1-4A* (pDM9) with all sites mutated to alanine or *iqg1-4E* (pDM15) with all sites mutated to glutamic acid (Table 2). To integrate *iqg1-4A* at the

Strain	Genotype	Source
KSY184	*MATa ade2-1 can1-100 his3-11,15 leu2-3112 trp1-1 ura3-1 IQG1-3HA::His3MX6*	Ko *et al.* (2007)
KSY286	*MATa ura3-1 his3-11,15 leu2-3112 lys2-801 trp1-1 Δbar1 ΔIQG1:LEU2 pGAL1-IQG1-myc, ura3*	This work
KSY378	*MATa ura3-1 his3-11,15 leu2-3112 lys2-801 trp1-1 Δbar1 ΔIQG1:LEU2 pGAL1-IQG1-myc, URA3 iqg1-4A-myc, HIS3 (pDM9)*	This work
KSY396	*MATa ura3-1 his3-11,15 leu2-3112 lys2-801 trp1-1 Δbar1 ΔIQG1:LEU2 pGAL1-IQG1-myc, URA3 iqg1-4E-myc, HIS3 (pDM15)*	This work
KSY472	*MATa ura3-1 his3-11,15 leu2-3112 lys2-801 trp1-1Δbar1 ΔIQG1:LEU2 pGAL1-IQG1-myc, ura3 (pRL170) iqg1-4A-myc, HIS3 (pDM9)*	This work
KSY473	*MATa ura3-1 his3-11,15 leu2-3112 lys2-801 trp1-1Δbar1 ΔIQG1:LEU2 pGAL1-IQG1-myc, ura3 (pRL170) iqg1-4E-myc, HIS3 (pDM15)*	This work
KSY482	*MATa cdc14-1 ura3 leu2 SIC1 2μ:LEU2*	This work
KSY496	*MATa ura3-1 his3-11,15 leu2-3112 lys2-801 trp1-1 Δbar1 ΔIQG1:LEU2 pGAL1-IQG1-myc, URA3 iqg1-4A-myc, HIS3 (pDM9) TUB1-mCherry :URA (pAK011)*	This work
KSY504	*MATa cdc14-1 ura3 leu2 GAL-SIC1ΔNT:URA (pFM160)*	This work
KSY508	*MATa ura3-1 his3-11,15 leu2-3112 lys2-801 trp1-1 Δbar1 ΔIQG1:LEU2 pGAL1-IQG1-myc, URA3 iqg1-4A-myc, HIS3 (pDM9) TUB1-mCherry:URA (pAK011) MYO1-GFP:TRP (pKT36)*	This work
KSY509	*MATa ura3 leu2 his3 trp1 ade2 Δbar1 GAL1-CDC14 (pKL1341)*	This work
KSY510	*MATa cdc14-1 ura3 leu2 ΔIQG1:LEU2 (pRL170) iqg1-4A, HIS3 (pDM9) GAL1-SIC1-ΔNT-myc:URA3 (pFM160)*	This work
KSY520	*MATa ura3-1 his3-11,15 leu2-3112 lys2-801 trp1-1Δbar1 ΔIQG1:LEU2 pGAL1-IQG1-myc, ura3 (pRL170) IQG1-myc, HIS3 (pTL12)*	This work
KSY522	*MATa ade2-1 can1-100 his3-11,15 leu2-3112 trp1-1 ura3-1 iqg1-4A-3HA::His3MX6*	This work
YKA830	*MATa leu2::GAL1-3HA-CDC14(C283S) ura3::IQG1-3FLAG:URA3*	This work
YKA832	*MATa leu2::GAL1-3HA-CDC14(C283S) ura3::IQG1^{3T}-3FLAG:URA3*	This work

The background for all was W303.

TABLE 1: Yeast strains used in this study.

Name	Genotype	Source
pKT36	*Myo1-GFP:TRP1* integrated with *Age*I	Shannon and Li (1999)
pTL12	*IQG1-myc CEN* plasmid *HIS3*	Lippincott and Li (1998b)
pDM9	*iqg1-4A-myc CEN* plasmid *HIS3*	This work
pDM15	*iqg1-4E-myc CEN* plasmid *HIS3*	This work
pFM160	*GAL1-SIC1-ΔNTmyc:URA3* integrated with *Eco*RV	Chin *et al.* (2012)
pKL1341	*GAL1-CDC14:HIS* integrated with *Nhe*I	Sanchez-Diaz *et al.* (2012)
pAK011	pRS306-mCherry-TUB1:*URA3* integrated with *Apa*I	Khmelinskii *et al.* (2007)
YEp13-SIC1	*SIC1:LEU2* 2μ plasmid	Luca *et al.* (2001)
pHIP082	*Iqg1-3A-3xFLAG:URA3*	This work
pMM1	*Iqg1-4A-3xFLAG:URA3* integrated with Afl*II*	This work

TABLE 2: Plasmids used in this study.

chromosomal locus, plasmid pHIP082 was used as template for site-directed mutagenesis using the primers to introduce the T299A mutation, and the resulting plasmid, pMM1, was sequenced to verify the mutation. pMM1 was cut with *Afl*II and transformed into KSY184, and URA+ transformants containing the integrated plasmid were then plated on 5-fluoroorotic acid media to select for recombination between the *IQG1-hemagglutinin* (*HA*) and *iqg1-4A-3xFLAG* alleles (Scherer and Davis, 1979). Genomic DNA from URA- colonies was sequenced to determine that KSY522 contained the *iqg1-4A-HA* allele.

Yeast transformation

Yeast transformations were performed by a modified lithium acetate method (Gietz *et al.*, 1992). After 30 min incubation at 30°C, 50 μl of dimethyl sulfoxide was added and mixed. Cells were plated on appropriate media and incubated at 30 or 25°C for 2–3 d.

Analysis of cell morphology

Strains KSY378, KSY396, and KSY520 have wild-type *IQG1* under the *GAL1*-inducible promoter, allowing wild-type *IQG1* to be shut off in the presence of glucose, and express *iqg1-4A*, *iqg1-4E*, and *IQG1* respectively, under the *IQG1* promoter. Cells were cultured overnight in 5 ml YPGR at 30°C. The cells were then diluted (1 ml into 5 ml) into YPGR (control) or YPD (experimental) media and were allowed to continuing growing at 30°C for 5–7 h. Cell morphology was then observed using an Olympus CH2 (Olympus Scientific Solutions Americas Corp., Waltham, MA) with objective EA40, numerical aperture (NA) 0.65. For each strain and treatment, 200 cells were counted and scored as chains if they contained three or more connected cell bodies. Experiments were repeated three times.

Zymolyase treatment was performed as described (Lippincott and Li, 1998b).

Collection of time points

To examine the timing of actin ring formation, KSY378 or KSY520 cells were grown overnight in 5 ml YPGR, diluted into 50 ml, and grown for 3 h at 30°C. The α mating factor was added to a final concentration of 100 µg/ml and cells incubated for additional 3 h to arrest cells in G1. The cells were then pelleted and washed three times with sterile water to remove α factor. They were then resuspended in 35 ml of YPD or YPGR. Time points were taken by removing 5 ml at 20, 40, 60, 80, and 100 min after resuspension into YPD or YPGR.

To examine the effect of Cdc14 overexpression on actin ring formation, strain KSY509 was grown overnight in 5 ml YPD at 30°C, and cells were pelleted and resuspended into YPD or YPGR with simultaneous addition of nocodazole at a final concentration of 5µg/ml and incubated for additional 2.5 h to arrest cells in mitosis.

To determine whether *cdc14-1* cells could make actin rings at the nonpermissive temperature when mitotic arrest was bypassed using *SIC1* expressed at high level using a 2µ plasmid, strain KSY482 was used (Tables 1 and 2). Cells were grown overnight in 5 ml YPD at room temperature (25°C). After resuspension into fresh YPD, nocodazole (5 µg/ml) was added and cells incubated for additional 2 h to arrest cells in mitosis. Cells were then placed at room temperature (control) and 37°C (experimental) for 90 min. A sample was collected before nocodazole was removed by washing cells twice with distilled H_2O. After resuspension in fresh medium, samples at 10- and 20-min time points were collected.

Strains KSY504 and KSY510, containing the temperature-sensitive *cdc14-1* allele and integrated *GAL1-SIC1ΔNT,* were grown overnight in 5 ml of YPD at room temperature, resuspended into YPGR (to express *SIC1* under the *GAL1* promoter) with nocodazole (5 µg/ml), and incubated for 90 min to arrest cells in mitosis. Cells were then placed in YPGR with nocodazole at 37°C for an additional 90 min to allow for inactivation of *cdc14-1*. A sample was collected before nocodazole was removed by washing twice with distilled H_2O. After resuspension in fresh medium, samples were collected at 10- and 20-min time points.

Immunofluorescence

Cells were fixed by addition of formaldehyde to 5% and rotation for 1 h at room temperature. Cells were then washed twice with sorbitol buffer (1 M sorbitol in 50 mM KPO_4, pH 7.5) to remove formaldehyde and stored at 4°C for up to 1 wk. Cells were permeabilized by Zymolyase treatment and then affixed to a 10-well microscope slide coated with polylysine. Cells were pipetted off, and the slide was allowed to air dry before being washed three times with 1 µg/ml bovine serum albumin in phosphate-buffered saline (Lippincott and Li, 1998b).

Cells were stained using primary antibody mouse anti-myc 9E10 (Covance, Princeton, NJ) and fluorescein isothiocyanate (FITC)–conjugated secondary antibody (Jackson ImmunoResearch Laboratories, West Grove, PA) as described (Lippincott and Li, 1998b). Actin staining using A568 phalloidin (Invitrogen, Thermo Fisher Scientific, Waltham, MA) was also performed as described (Lippincott and Li, 1998b). Mounting solution containing 1 µg/ml DAPI was added before the coverslip was sealed to the slide.

Images were captured using an Olympus IX51 inverted microscope at 1000× total magnification using a UPLSAPO 100×/NA 1.4 objective. A BrightLine DA/FI/TX-3×3M-a triple-band Sedat Filter set was used (Semrock, Rochester, NY). Images were captured with a Hamamatsu ORCA285 charge-coupled device (CCD) camera (Hamamatsu, Japan). A Prior motorized *Z*-drive was used to capture image stacks of 20 *Z*-planes in 0.2-µm steps (Prior Scientific, Rockland, MA). Shutters, filters, and camera were controlled using SlideBook software (Intelligent Imaging Innovations, Denver, CO), and this software was used to perform deconvolution of the image stacks and create projection images.

Yeast protein extracts

The protocol used is a modified version of Rigaut *et al*. (1999). KSY286, KSY472, KSY473, and KSY520 cells were grown overnight in YPGR and then diluted into YPD and arrested with α factor for 3 h. Cells were washed three times in sterile water and then released from α factor for 60 min before cells were pelleted and resuspended in 100 µl U of buffer (50 mM 4-(2-hydroxyethyl)-1-piperazineethanesulfonic acid, pH 7.5, 100 mM KCl, 3 mM $MgCl_2$, 1 mM ethylene glycol tetraacetic acid) plus protease inhibitors (0.5 µg/ml pepstatin, chymostatin, antipain, aprotinin, leupeptin) plus phenylmethylsulfonyl fluoride (1 mM). For cell lysis, 0.3 mg of acid-washed glass beads were added to cells and chilled on ice for 10 min. The cell suspension was vortexed five times (1 min on vortexer at maximum speed and 1 min on ice). The cell suspension was then centrifuged at 4°C at a relative centrifugal force of 16,000 × *g* for 5 min. The supernatant containing soluble protein was removed and the protein concentration determined using a NanoDrop 1000 (Thermo Scientific). An equal volume of 2× Laemmli sample buffer was added, and tubes were boiled for 5 min and then centrifuged for 5 min and frozen until use.

Western blotting

Protein samples were separated on 7.5 or 12.5% SDS–PAGE gels and then transferred to nitrocellulose and blocked in 5% milk in Tris-buffered saline/Tween before antibody staining. Mouse monoclonal anti-myc 9E10 (Covance) and mouse monoclonal anti-actin mAbGEa (Thermo Scientific Pierce) were used at 1:1000 dilution. Mouse anti-FLAG M2 (Sigma-Aldrich, St. Louis, MO) was used at 1:1000 dilution. EZview anti-HA-7 agarose resin (Sigma-Aldrich) was used for substrate trap coIP experiments. Donkey anti-mouse secondary antibody conjugated to horseradish peroxidase (Jackson ImmunoResearch Laboratories) was used at 1:5000 concentration. The blot was then developed using an ECL kit (SuperSignal West Pico Chemiluminescent Substrate; Thermo Scientific) and imaged and analyzed on a Bio-Rad ChemiDoc MP system with Image Lab software (Bio-Rad Laboratories, Hercules, CA).

Phosphatase assays and coimmunoprecipitation

Recombinant Cdc14 was purified and assayed using synthetic phosphopeptide substrates (GenScript, Piscataway, NJ) as described (Bremmer *et al*., 2012). Peptide sequences were SG(pS)PSKPGNN (Iqg1pS7), EY(pS)PIKNKSL (Iqg1pS354), HY(pSP)MRRERM (Iqg1pS404), YY(pS)PTISKYL (Iqg1pS365), DF(pS)PVHKSKF (Iqg1pS1347), and LI(pT)PRKNITD (Iqg1pT299), where pS and pT are phosphoserine and phosphothreonine, respectively. Crude phosphopeptides were purified using Sep-Pak C18 cartridges (Waters Corporation, Milford, MA). Substrate trap coIP assays were performed as described (Eissler *et al*., 2014).

Live-cell imaging

KSY508 cells were grown overnight and placed on agarose pads made by melting 0.2 g of agarose in 1 ml -TRP media (Waddle *et al*., 1996). The cells were then viewed using the Olympus Inverted Epifluorescent Microscope with a 100× Plan Apo/NA 1.4 DIC

Objective. An FITC filter (EX 482/35 506DM EM 536/40) was used (Brightline). Images were captured with a Hamamatsu ORCA285 CCD camera. Shutters, filters, and camera were controlled using SlideBook software.

ACKNOWLEDGMENTS

We acknowledge the labs of Rong Li, Alberto Sanchez-Diaz, Frank Luca, John Pringle, and Elmar Schiebel for generously providing yeast strains and plasmids. We thank the sponsors and organizers of the Midwest Yeast Meeting at Northwestern University, which led to this collaboration. We also thank Hsiu-Jen (Sharen) Wang and Shakila Tobwala in Nuran Ercal's lab for help with the Bio-Rad imager. K.B.S. and D.P.M. thank the Biological Sciences Department for support.

REFERENCES

Bardin AJ, Amon A (2001). Men and sin: what's the difference? Nat Rev Mol Cell Biol 2, 815–826.

Bembenek J, Kang J, Kurischko C, Li B, Raab JR, Belanger KD, Luca FC, Yu H (2005). Crm1-mediated nuclear export of Cdc14 is required for the completion of cytokinesis in budding yeast. Cell Cycle 4, 961–971.

Bi E (2001). Cytokinesis in budding yeast: the relationship between actomyosin ring function and septum formation. Cell Struct Funct 26, 529–537.

Bi E, Maddox P, Lew DJ, Salmon ED, McMillan JN, Yeh E, Pringle JR (1998). Involvement of an actomyosin contractile ring in Saccharomyces cerevisiae cytokinesis. J Cell Biol 142, 1301–1312.

Blom N, Gammeltoft S, Brunak S (1999). Sequence- and structure-based prediction of eukaryotic protein phosphorylation sites. J Mol Biol 294, 1351–1362.

Bloom J, Cristea IM, Procko AL, Lubkov V, Chait BT, Snyder M, Cross FR (2011). Global analysis of Cdc14 phosphatase reveals diverse roles in mitotic processes. J Biol Chem 286, 5434–5445.

Boyne JR, Yosuf HM, Bieganowski P, Brenner C, Price C (2000). Yeast myosin light chain, Mlc1p, interacts with both IQGAP and class II myosin to effect cytokinesis. J Cell Sci 113, 4533–4543.

Bremmer SC, Hall H, Martinez JS, Eissler CL, Hinrichsen TH, Rossie S, Parker LL, Hall MC, Charbonneau H (2012). Cdc14 phosphatases preferentially dephosphorylate a subset of cyclin-dependent kinase (Cdk) sites containing phosphoserine. J Biol Chem 287, 1662–1669.

Chen JS, Broadus MR, McLean JR, Feoktistova A, Ren L, Gould KL (2013). Comprehensive proteomics analysis reveals new substrates and regulators of the fission yeast clp1/cdc14 phosphatase. Mol Cell Proteomics 12, 1074–1086.

Chin CF, Bennett AM, Ma WK, Hall MC, Yeong FM (2012). Dependence of Chs2 ER export on dephosphorylation by cytoplasmic Cdc14 ensures that septum formation follows mitosis. Mol Biol Cell 23, 45–58.

Clifford DM, Wolfe BA, Roberts-Galbraith RH, McDonald WH, Yates JR 3rd, Gould KL (2008). The Clp1/Cdc14 phosphatase contributes to the robustness of cytokinesis by association with anillin-related Mid1. J Cell Biol 181, 79–88.

Eissler CL, Mazon G, Powers BL, Savinov SN, Symington LS, Hall MC (2014). The Cdk/Cdc14 module controls activation of the Yen1 holliday junction resolvase to promote genome stability. Mol Cell 54, 80–93.

Epp JA, Chant J (1997). An IQGAP-related protein controls actin-ring formation and cytokinesis in yeast. Curr Biol 7, 921–929.

Fishkind DJ, Wang YL (1995). New horizons for cytokinesis. Curr Opin Cell Biol 7, 23–31.

Ganem NJ, Storchova Z, Pellman D (2007). Tetraploidy, aneuploidy and cancer. Curr Opin Genet Dev 17, 157–162.

Gietz D, St Jean A, Woods RA, Schiestl RH (1992). Improved method for high efficiency transformation of intact yeast cells. Nucleic Acids Res 20, 1425.

Holt LJ, Tuch BB, Villen J, Johnson AD, Gygi SP, Morgan DO (2009). Global analysis of Cdk1 substrate phosphorylation sites provides insights into evolution. Science 325, 1682–1686.

Hwa Lim H, Yeong FM, Surana U (2003). Inactivation of mitotic kinase triggers translocation of MEN components to mother-daughter neck in yeast. Mol Biol Cell 14, 4734–4743.

Jaspersen SL, Charles JF, Tinker-Kulberg RL, Morgan DO (1998). A late mitotic regulatory network controlling cyclin destruction in Saccharomyces cerevisiae. Mol Biol Cell 9, 2803–2817.

Khmelinskii A, Lawrence C, Roostalu J, Schiebel E (2007). Cdc14-regulated midzone assembly controls anaphase B. J Cell Biol 177, 981–993.

Ko N, Nishihama R, Tully GH, Ostapenko D, Solomon MJ, Morgan DO, Pringle JR (2007). Identification of yeast IQGAP (Iqg1p) as an anaphase-promoting-complex substrate and its role in actomyosin-ring-independent cytokinesis. Mol Biol Cell 18, 5139–5153.

Korinek WS, Bi E, Epp JA, Wang L, Ho J, Chant J (2000). Cyk3, a novel SH3-domain protein, affects cytokinesis in yeast. Curr Biol 10, 947–950.

Kuilman T, Maiolica A, Godfrey M, Scheidel N, Aebersold R, Uhlmann F (2015). Identification of Cdk targets that control cytokinesis. EMBO J 34, 81–96.

Li CR, Wang YM, Wang Y (2008). The IQGAP Iqg1 is a regulatory target of CDK for cytokinesis in Candida albicans. EMBO J 27, 2998–3010.

Lippincott J, Li R (1998a). Dual function of Cyk2, a cdc15/PSTPIP family protein, in regulating actomyosin ring dynamics and septin distribution. J Cell Biol 143, 1947–1960.

Lippincott J, Li R (1998b). Sequential assembly of myosin II, an IQGAP-like protein, and filamentous actin to a ring structure involved in budding yeast cytokinesis. J Cell Biol 140, 355–366.

Lippincott J, Shannon KB, Shou W, Deshaies RJ, Li R (2001). The Tem1 small GTPase controls actomyosin and septin dynamics during cytokinesis. J Cell Sci 114, 1379–1386.

Luca FC, Mody M, Kurischko C, Roof DM, Giddings TH, Winey M (2001). Saccharomyces cerevisiae Mob1p is required for cytokinesis and mitotic exit. Mol Cell Biol 21, 6972–6983.

Luca FC, Winey M (1998). MOB1, an essential yeast gene required for completion of mitosis and maintenance of ploidy. Mol Biol Cell 9, 29–46.

McCollum D, Gould KL (2001). Timing is everything: regulation of mitotic exit and cytokinesis by the MEN and SIN. Trends Cell Biol 11, 89–95.

Meitinger F, Palani S, Pereira G (2012). The power of MEN in cytokinesis. Cell Cycle 11, 219–228.

Meitinger F, Petrova B, Lombardi IM, Bertazzi DT, Hub B, Zentgraf H, Pereira G (2010). Targeted localization of Inn1, Cyk3 and Chs2 by the mitotic-exit network regulates cytokinesis in budding yeast. J Cell Sci 123, 1851–1861.

Mendes Pinto I, Rubinstein B, Kucharavy A, Unruh JR, Li R (2012). Actin depolymerization drives actomyosin ring contraction during budding yeast cytokinesis. Dev Cell 22, 1247–1260.

Menssen R, Neutzner A, Seufert W (2001). Asymmetric spindle pole localization of yeast Cdc15 kinase links mitotic exit and cytokinesis. Curr Biol 11, 345–350.

Mocciaro A, Schiebel E (2010). Cdc14: a highly conserved family of phosphatases with non-conserved functions? J Cell Sci 123, 2867–2876.

Mohl DA, Huddleston MJ, Collingwood TS, Annan RS, Deshaies RJ (2009). Dbf2-Mob1 drives relocalization of protein phosphatase Cdc14 to the cytoplasm during exit from mitosis. J Cell Biol 184, 527–539.

Naylor SG, Morgan DO (2014). Cdk1-dependent phosphorylation of Iqg1 governs actomyosin ring assembly prior to cytokinesis. J Cell Sci 127, 1128–1137.

Nishihama R, Schreiter JH, Onishi M, Vallen EA, Hanna J, Moravcevic K, Lippincott MF, Han H, Lemmon MA, Pringle JR, Bi E (2009). Role of Inn1 and its interactions with Hof1 and Cyk3 in promoting cleavage furrow and septum formation in S. cerevisiae. J Cell Biol 185, 995–1012.

Oh Y, Chang KJ, Orlean P, Wloka C, Deshaies R, Bi E (2012). Mitotic exit kinase Dbf2 directly phosphorylates chitin synthase Chs2 to regulate cytokinesis in budding yeast. Mol Biol Cell 23, 2445–2456.

Palani S, Meitinger F, Boehm ME, Lehmann WD, Pereira G (2012). Cdc14-dependent dephosphorylation of Inn1 contributes to Inn1-Cyk3 complex formation. J Cell Sci 125, 3091–3096.

Pollard TD (2010). Mechanics of cytokinesis in eukaryotes. Curr Opin Cell Biol 22, 50–56.

Queralt E, Uhlmann F (2008). Cdk-counteracting phosphatases unlock mitotic exit. Curr Opin Cell Biol 20, 661–668.

Rigaut G, Shevchenko A, Rutz B, Wilm M, Mann M, Seraphin B (1999). A generic protein purification method for protein complex characterization and proteome exploration. Nat Biotechnol 17, 1030–1032.

Sanchez-Diaz A, Nkosi PJ, Murray S, Labib K (2012). The Mitotic Exit Network and Cdc14 phosphatase initiate cytokinesis by counteracting CDK phosphorylations and blocking polarised growth. EMBO J 31, 3620–3634.

Satterwhite LL, Pollard TD (1992). Cytokinesis. Curr Opin Cell Biol 4, 43–52.

Scherer S, Davis RW (1979). Replacement of chromosome segments with altered DNA sequences constructed in vitro. Proc Natl Acad Sci USA 76, 4951–4955.
Shannon KB (2012). IQGAP family members in yeast, Dictyostelium, and mammalian cells. Int J Cell Biol 2012, 894817.
Shannon KB, Li R (1999). The multiple roles of Cyk1p in the assembly and function of the actomyosin ring in budding yeast. Mol Biol Cell 10, 283–296.
Shannon KB, Li R (2000). A myosin light chain mediates the localization of the budding yeast IQGAP-like protein during contractile ring formation. Curr Biol 10, 727–730.
Shou W, Seol JH, Shevchenko A, Baskerville C, Moazed D, Chen ZW, Jang J, Shevchenko A, Charbonneau H, Deshaies RJ (1999). Exit from mitosis is triggered by Tem1-dependent release of the protein phosphatase Cdc14 from nucleolar RENT complex. Cell 97, 233–244.
Stockstill KE, Park J, Wille R, Bay G, Joseph A, Shannon KB (2013). Mutation of Hof1 PEST motif phosphorylation sites leads to retention of Hof1 at the bud neck and a decrease in the rate of myosin contraction. Cell Biol Int 37, 314–325.
Storchova Z, Kuffer C (2008). The consequences of tetraploidy and aneuploidy. J Cell Sci 121, 3859–3866.
Tian C, Wu Y, Johnsson N (2014). Stepwise and cooperative assembly of a cytokinetic core complex in Saccharomyces cerevisiae. J Cell Sci 127, 3614–3624.
Tolliday N, VerPlank L, Li R (2002). Rho1 directs formin-mediated actin ring assembly during budding yeast cytokinesis. Curr Biol 12, 1864–1870.
Uhlmann F, Bouchoux C, Lopez-Aviles S (2011). A quantitative model for cyclin-dependent kinase control of the cell cycle: revisited. Philos Trans R Soc Lond B Biol Sci 366, 3572–3583.
Vallen EA, Caviston J, Bi E (2000). Roles of Hof1p, Bni1p, Bnr1p, and Myo1p in cytokinesis in Saccharomyces cerevisiae. Mol Biol Cell 11, 593–611.
Visintin R, Craig K, Hwang ES, Prinz S, Tyers M, Amon A (1998). The phosphatase Cdc14 triggers mitotic exit by reversal of Cdk-dependent phosphorylation. Mol Cell 2, 709–718.
Visintin R, Hwang ES, Amon A (1999). Cfi1 prevents premature exit from mitosis by anchoring Cdc14 phosphatase in the nucleolus. Nature 398, 818–823.
Waddle JA, Karpova TS, Waterston RH, Cooper JA (1996). Movement of cortical actin patches in yeast. J Cell Biol 132, 861–870.
White CD, Erdemir HH, Sacks DB (2012). IQGAP1 and its binding proteins control diverse biological functions. Cell Signal 24, 826–834.